DL/SCI/TM65E

technical memorandum

Daresbury Laborator

DL/SCI/TM65E

LAUE DIFFRACTION AT HIGH TEMPERATURES AND PRESSURES

by

B. JENKINS and S.M. CLARK, SERC Daresbury Laboratory.

MARCH, 1990

Science and Engineering Research Council
DARESBURY LABORATORY
Daresbury, Warrington WA4 4AD

1 Background Theory of Laue diffraction

1.1 Introduction

The Laue method is the oldest of the X-ray diffraction methods. A collimated beam of continuous spectrum falls upon a fixed single crystal. For each set of planes *hkl*, the spacing *d(hkl)* and the Bragg angle *θ(hkl)* are fixed. A reflected beam will be produced by the component wavelength of the continuous spectrum which satisfies the Bragg law. The different reflected beams have different wavelengths.

There are two possible variations of the Laue method depending on the experimental arrangement used. In the transmission method the film is placed behind the crystal so as to record the beams diffracted in the forward direction, i.e. the beams are partially transmitted through the crystal.

In the back reflection method the film is positioned between the crystal and the X-ray source, the beam passing through a hole in the film. The beams diffracted backwards are recorded.

Only the transmission method is considered here.

1.2 Geometry of the Laue Pattern

1.2.1 The Reciprocal Lattice

The reciprocal lattice is a powerful concept introduced by Ewald in 1921. It has become an indispensable tool in the solution of many crystallographic problems. It is useful in understanding diffraction effects such as those involving diffuse scattering at non Bragg angles which the Bragg law cannot account for.

The reciprocal lattice is constructed from the unit cell of the real space lattice which has vectors **a**,**b** and **c**. The corresponding reciprocal lattice unit cell has vectors **a***, **b*** and **c*** where;

$$\mathbf{a}* = \frac{1}{V}(\mathbf{bxc}) \qquad a* = \frac{|\mathbf{bxc}|}{V}$$

$$\mathbf{b}* = \frac{1}{V}(\mathbf{cxa}) \qquad b* = \frac{|\mathbf{cxa}|}{V}$$

$$\mathbf{c}* = \frac{1}{V}(\mathbf{axb}) \qquad c* = \frac{|\mathbf{axb}|}{V}$$

(V=vol. of real space unit cell)

The reciprocal lattice array of points describes the crystal completely. Each point represents the orientation and spacing of a set of *hkl* planes.

1. A vector $\mathbf{H}_{hkl}$ drawn from the origin of the reciprocal lattice to any point in it with coordinates *hkl* is perpendicular to the plane in the crystal lattice whose Miller indices are *hkl*. The vector in terms of its coordinates is;

$$\mathbf{H}_{hkl} = h\mathbf{a}* + k\mathbf{b}* + l\mathbf{c}*$$

2. The length of $\mathbf{H}_{hkl}$ is the reciprocal of the spacing d of the (hkl) planes .

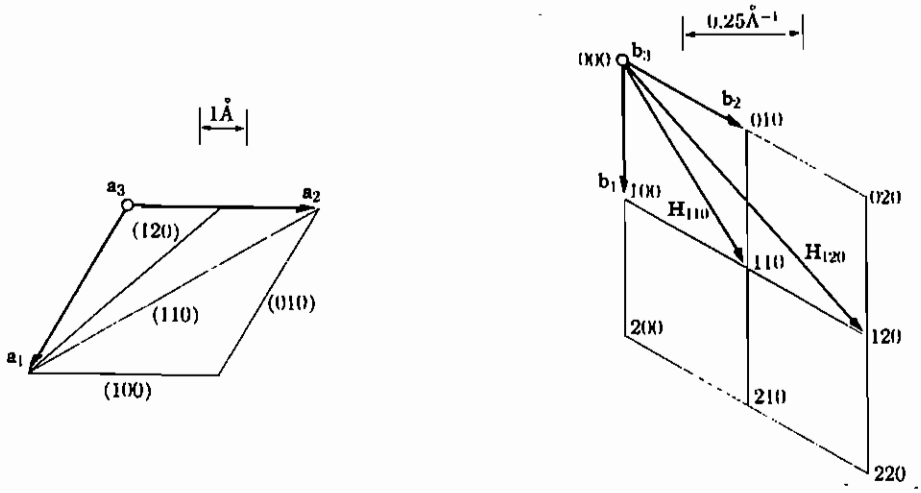

Fig. 1 Crystal lattice Reciprocal lattice

1.2.2 Diffraction and the Reciprocal Lattice

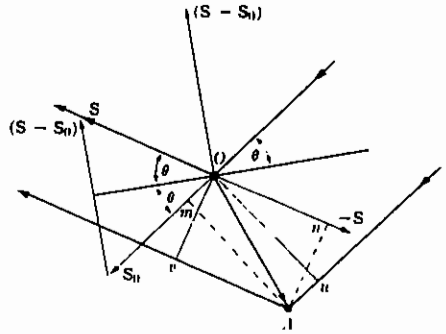

Fig. 2 X-ray scattering by atoms at A and O

In Fig. 2 atom O is at the origin, atom A is at $p\mathbf{a}$, $q\mathbf{b}$,$r\mathbf{c}$. Thus OA=$p\mathbf{a}$+$q\mathbf{b}$+ $r\mathbf{c}$ (where p,q and r are integers). Incident and diffracted beams of wavelength λ are represented by unit vectors $\mathbf{S}$ and $\mathbf{S}_0$ respectively. δ is the path difference between rays scattered by O and A;

$$\begin{aligned}\delta &= uA + Av \\ &= Om + On \\ &= \mathbf{S}_0.OA + (-\mathbf{S}).OA \\ &= -OA.(\mathbf{S} - \mathbf{S}_0)\end{aligned}$$

Corresponding path difference in radians is;

$$\begin{aligned}\phi &= \frac{2\pi\delta}{\lambda} \\ &= -2\pi\left(\frac{\mathbf{S} - \mathbf{S}_0}{\lambda}\right).OA\end{aligned}$$

Expressing $(\mathbf{S} - \mathbf{S}_0)/\lambda$ as a vector in the reciprocal lattice;

$$\left(\frac{\mathbf{S} - \mathbf{S}_0}{\lambda}\right) = h\mathbf{a}* + k\mathbf{b}* + l\mathbf{c}*$$

and $\phi = -2\pi(h\mathbf{a}* + k\mathbf{b}* + l\mathbf{c}*).(p\mathbf{a} + q\mathbf{b} + r\mathbf{c}) = -2\pi(hp + kq + lr)$

Diffraction occurs only if ϕ is an integral multiple of 2π. This occurs only if hkl are integers. Therefore the condition for diffraction is that the vector $(\mathbf{S} - \mathbf{S}_0)/\lambda$ end on a point in the reciprocal lattice;

$$\frac{\mathbf{S} - \mathbf{S}_0}{\lambda} = \mathbf{H}_{hkl} = h\mathbf{a}* + k\mathbf{b}* + l\mathbf{c}* \qquad (1)$$

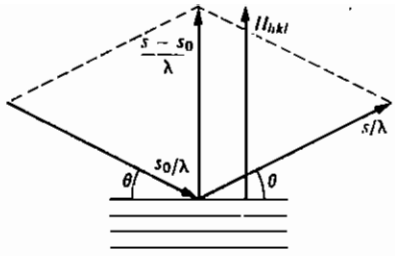

Fig. 3 Relations involved in the vector representation of the Bragg law

Fig. 3 shows that $(\mathbf{S} - \mathbf{S_0})$ bisects the angle between $\mathbf{S_0}$ and $\mathbf{S}$. The diffracted beams can be considered as being reflected from a set of planes perpendicular to the planes (hkl).

Equation (1) states that $(\mathbf{S} - \mathbf{S_0})$ is parallel to $\mathbf{H}_{hkl}$ which is perpendicular to the planes (hkl). If θ is the angle between $\mathbf{S}$,(or $\mathbf{S_0}$) and these planes;

$$(|\mathbf{S}| - |\mathbf{S_0}|) = 2sin\theta$$

therefore;

$$\frac{2sin\theta}{\lambda} = \frac{(|\mathbf{S}| - |\mathbf{S_0}|)}{\lambda} = |\mathbf{H}_{hkl}| = 1/d$$

$$\lambda = 2dsin\theta$$

which is the usual form of the Bragg law.

1.2.3 The Sphere of Reflection

The sphere of reflection (or Ewald sphere) is an extremely useful means of representing the satisfying of the Bragg law. Fig. 4 shows a 2 dimensional representation of the reciprocal lattice. A sphere of radius $1/\lambda$ centred on the initial end of vector $\mathbf{S_0}/\lambda$ passes through the origin of the reciprocal lattice. Vector $\mathbf{S_0}/\lambda$ represents the primary beam. Any reciprocal lattice point falling on the surface of the sphere represents a set of planes hkl which satisfies the Bragg law. Vector $\mathbf{S}/\lambda$ represents the direction the diffracted beam will take.

Diffraction occurs in the Laue method because of the continuous range of wavelengths contained in the incident beam. i.e. the Bragg law is satisfied due to the continuously varying radius of the sphere of reflection. A reflection will be produced by any set of planes whose reciprocal lattice point lies between the spheres of reflection of radius $1/\lambda_{max}$ and $1/\lambda_{min}$.

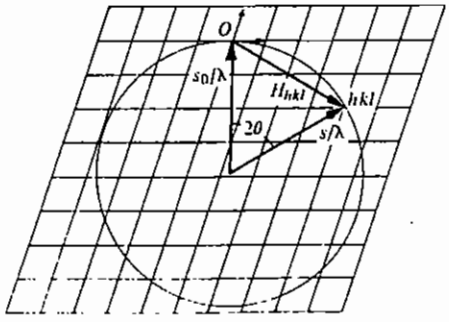

Fig. 4 2 dimensional representation of the sphere of reflection in the reciprocal lattice. The Bragg law is satisfied for the point hkl falling on the surface of the sphere

1.2.4 The Transmission Laue Pattern

Inspection of a Laue pattern shows the diffraction spots to be lying on sets of ellipses or 'lunes' which pass through a centre spot. This will occur if the crystal is oriented along one of its axes or not. All spots on an ellipse are reflections from planes *hkl* belonging to the same zone *uvw*.

Planes of a zone are all parallel to one line called the zone axis. The zone (set of planes) is specified by giving the indices of the zone axis. If the plane *hkl* belongs to the zone whose axis is [*uvw*] then **H** (*hkl*) must be perpendicular to [*uvw*]. Expressing the zone axis as a vector in the crystal and **H**(*hkl*) as a vector in the reciprocal lattice;

$$\mathbf{A}(hkl) = u\mathbf{a} + v\mathbf{b} + w\mathbf{c}$$

$$\mathbf{H}(hkl) = h\mathbf{a}* + k\mathbf{b}* + l\mathbf{c}*$$

if the two vectors are perpendicular;

$$(u\mathbf{a} + v\mathbf{b} + w\mathbf{c}).(h\mathbf{a}* + k\mathbf{b}* + l\mathbf{c}*) = 0$$

$$hu + kv + lw = 0$$

from eqn. 1 the direction of the diffracted beam from planes *hkl* is;

$$\mathbf{S} = \mathbf{S}_0 + \lambda\mathbf{H}(hkl)$$

if the plane belongs to the zone *uvw*, by formation of the scalar product with **A**(*uvw*) on both sides;

$$\mathbf{S}.\mathbf{A}(uvw) = \mathbf{S}_0.\mathbf{A}(uvw) + \lambda\mathbf{H}(hkl).\mathbf{A}(uvw)$$

Since $\lambda\mathbf{H}(hkl).\mathbf{A}(uvw) = 0$, this shows that ϕ_0, the angle between the primary beam and zone axis **A**(*uvw*) is equal to ϕ, the angle between the reflected beam and zone axis **A**(*uvw*) from any plane *hkl* belonging to the zone *uvw*.

Fig. 5 shows that reflections for all planes with zone axis **A**(*uvw*) form elements of a cone with the primary beam as one element and **A**(*uvw*) as the cone axis. The intersection of the cone with the primary beam with the film gives the ellipses seen on a transmission Laue pattern.

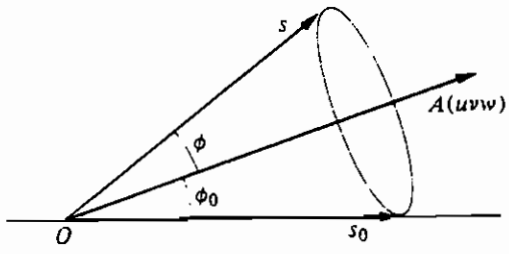

Fig. 5 The cone with zone axis **A**(*uvw*) showing the location of Laue spots on the film. The conic surface contains all reflected beams belonging to the zone *uvw*.

1.3 Intensities of Diffracted Beams

1.3.1 Scattering by an atom

Fig. 6 represents scattering from electrons confined to a small atomic volume. The incident beam has amplitude E_0, is polarised in the plane of the paper and is represented by unit vector

$\mathbf{s}_0$. The electrons are represented by vector $\mathbf{r}_n$ from the centre O. Scattering towards P at a large distance R from O is represented by unit vector $\mathbf{s}$.

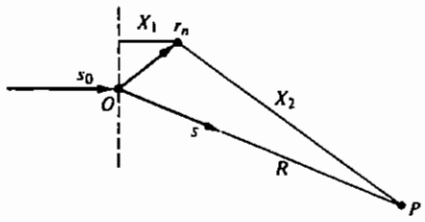

Fig. 6 Scattering by a group of electrons at positions $\mathbf{r}_n$

In terms of a wavefront through O, the usual expression for a travelling wave gives the instanteous value of the electric field acting on electron n as;

$$\epsilon_0 = E_0 cos\left(2\pi\nu t - \frac{2\pi X_1}{\lambda}\right)$$

Multiplying by the classical factor for an electron with the total path length as $X_1 + X_2$ gives the magnitude and phase of the scattered beam at P due to n as;

$$\epsilon_0 = \frac{E_0 e^2}{mc^2 X_2} cos\left[2\pi\nu t - \frac{2\pi}{\lambda}(X_1 + X_2)\right]$$

As the source and point of observation are at large distances compared to $|\mathbf{r}_n|$, we make plane wave approximations;

$$X_2 \rightarrow R \text{ and } X_1 + X_2 \rightarrow \mathbf{r}_n.\mathbf{s}_0 + R - \mathbf{r}_n.\mathbf{s} = R - (\mathbf{s} - \mathbf{s}_0).\mathbf{r}_n$$

On substituting for path lengths and expressed in terms of the complex exponential, the sum of the instantaneous fields at P is given by

$$\epsilon = \frac{E_0 e^2}{mc^2 R} e^{2\pi i[\nu t - (R/\lambda)]} \sum_n e^{(2\pi i/\lambda)(\mathbf{S}-\mathbf{S}_0).\mathbf{r}_n}$$

Theory and experiment predict two kinds of scattering: (a) unmodified scattering (same wavelength) and (b) Compton modified scattering (longer wavelength). To calculate the unmodified scattering from an atom which gives rise to the Bragg reflections, each electron is considered a diffuse cloud of negative charge characterized by a charge density ρ expressed in electron units. To obtain the total amplitude of unmodified scattering from an electron it is necessary to integrate over the volume occupied by the electron whilst giving due consideration to the phase of each contributing element, ρdV (ratio of change in volume dV to the charge of one electron). Considering charge elements ρdV at positions $\mathbf{r}$ the instantaneous value of electric field is given by

$$\epsilon_e = \frac{E_0 e_2}{mc^2 R} e^{2\pi i(\nu t - (r/\lambda)} \int e^{2\pi i/\lambda)(\mathbf{S}-\mathbf{S}_0).\mathbf{r}} \rho dV$$

The quantity represented by the integral is called the scattering factor per electron f_e. It is the amplitude of unmodified scattering per electron expressed in electron units.

$$f_e = \int e^{(2\pi i/\lambda)(\mathbf{S}-\mathbf{S}_0).\mathbf{r}} \rho dV$$

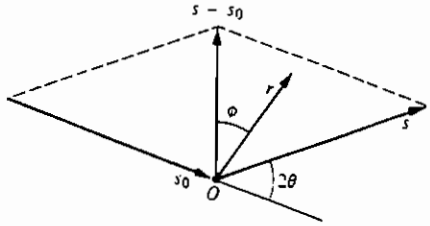

Fig. 7 Relation between $(s - s_0)$ and r vectors.

A simple expression is obtained for f_e by assuming spherical symmetry for charge distribution $\rho = \rho(r)$, taking the origin at the centre of the atom and making use of the quantities shown in figure 7

$$(s - s_0).r = 2sin\theta r cos\phi$$

let

$$k = \frac{4sin\theta}{\lambda}$$

then

$$f_e = \int_{r=0}^{\infty}\int_{\phi=0}^{\infty} e^{ikrcos\phi}\rho(r)2\pi r^2 sin\phi \; d\theta \; dr$$

$$f_e = \int_0^{\infty} 4\pi r^2 \rho(r)\frac{sin\, kr}{kr}dr$$

For an atom containing more than one electron, the amplitude of unmodified scattering per atom is the sum of the amplitudes per electron

$$f = \sum_n \int_0^{\infty} 4\pi r^2 \rho_n(r)\frac{sin\, kr}{kr}dr$$

The quantity f is an important factor in X-ray diffraction theory and is called the atomic scattering factor.

1.4 Crystal Diffraction

1.4.1 Intensity From A Small Crystal

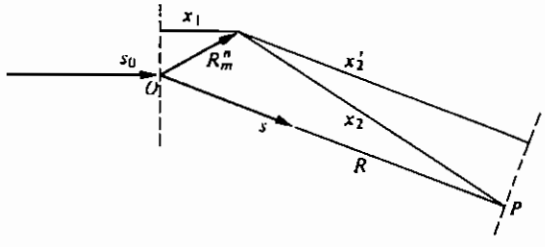

Fig. 8 Diffraction of primary beam by crystal at O.

For the diagram shown above the position of the atom of type n in unit cell $m_1m_2m_3$ is given by the vector $\mathbf{R}_m^n = m_1\mathbf{a}_1 + m_2\mathbf{a}_2 + m_3\mathbf{a}_3 + \mathbf{r}_n$. The instantaneous value of the electric field at P the point of observation due to the unmodified scattering from the atom is given by

$$\epsilon_p = \frac{E_0e^2}{mc^2R}f_n cos\left[2\pi\nu t - \frac{2\pi}{\lambda}(x_1 + x_2)\right]$$

Assuming the crystal small relative to R, and making plane wave approximations $(x_1 + x_2) \rightarrow (x_1 + x_2')$

$$\epsilon_p = \frac{E_0 e^2}{mc^2 R} f_n e^{i\{2\pi\nu t - (2\pi/\lambda)[R - (\mathbf{S}-\mathbf{S}_0)\cdot(m_1\mathbf{a}_1 + m_2\mathbf{a}_2 + m_3\mathbf{a}_3 + \mathbf{r}_n)]\}}$$

At the point of observation the resultant field is obtained by summing over n to include all the atoms in a unit cell and over $m_1 m_2 m_3$ to include all the unit cells. Considering a parallelpipedon $N_1 a_1 \times N_2 a_2 \times N_3 a_3$, the instantaneous field is given by

$$\epsilon_p = \frac{E_0 e^2}{mc^2 R} e^{2\pi i[\nu t - (R/\lambda)]} \sum_n f_n e^{(2\pi i/\lambda)(\mathbf{S}-\mathbf{S}_0)\cdot\mathbf{r}_n} \sum_{m_1=0}^{N_1-1} e^{(2\pi i/\lambda)(\mathbf{S}-\mathbf{S}_0)\cdot m_1\mathbf{a}_1}$$

$$\times \sum_{m_2=0}^{N_2-1} e^{(2\pi i/\lambda)(\mathbf{S}-\mathbf{S}_0)\cdot m_2\mathbf{a}_2} \sum_{m_3=0}^{N_3-1} e^{(2\pi i/\lambda)(\mathbf{S}-\mathbf{S}_0)\cdot m_3\mathbf{a}_3}$$

Summing over n involves the positions $\mathbf{r}_n$ of the different atoms in the unit cell and consequently it varies from structure to structure. It is called the structure factor and designated F where

$$F = \sum_n f_n e^{(2\pi i/\lambda)(\mathbf{S}-\mathbf{S}_0)\cdot\mathbf{r}_n}$$

Since the atomic positions appear only in the structure factor it plays a very important part in the determination of crystal structures.

1.5 Fourier Series Representation of the Electron Density

An alternative to representing a crystalline structure by atoms is by a continuous electron density where atoms appear as concentrations in this density. This method introduces a continuous electron density function $\rho(xyz)$ expressed in electrons per unit volume. The function is periodic in three dimensions and can be expressed by a triple Fourier series with axes x, y, z and period lengths a, b, c, the unit cell parameters. The densities at x, y, z and $x+n_1 a, y+n_2 b, z+n_3 c$ are the same where n_1, n_2 and n_3 are integers. The electron density function is given by

$$\rho(xyz) = \sum_{-\infty}^{\infty}\sum_{-\infty}^{\infty}\sum_{-\infty}^{\infty} A_{hkl} cos(2\pi hx/a + 2\pi ky/b + 2\pi lz/c + \alpha_{hkl})$$

Where the A_{hkl} values are the amplitudes of the cosine terms and the α_{hkl} values are their phases. It is necessary to use complex quantities in order to put the relationship in a symmetrical form

$$\rho(x, y, z) = \sum_{-\infty}^{\infty}\sum_{-\infty}^{\infty}\sum_{-\infty}^{\infty} A'_{hkl} e^{2\pi i(hx/a + ky/b + lz/c)}$$

where A' is complex. Complex quantities are necessary to include cases where phase change on scattering must be taken into account. In the case where all matter scatters with the same phase change, ρ is everywhere real. In this case A'_{hkl} and $A'_{\bar{h}\bar{k}\bar{l}}$ are conjugate. Since there is a constant distribution in the unit cell, the waves scattered from points must be integrated instead of summed as in the previous expression given for the structure factor

$$F_{h'k'l'} = \int_{-a/2}^{a/2}\int_{-b/2}^{b/2}\int_{-c/2}^{c/2} \rho(xyz) e^{2\pi i[h'(x/a) + k'(y/b) + l'(z/c)]} dV$$

Allowing for axes which are not orthogonal, by proportion

$$\frac{dV}{dxdydz} = \frac{V}{abc}$$

and

$$F_{h'k'l'} = \int_{-a/2}^{a/2}\int_{-b/2}^{b/2}\int_{-c/2}^{c/2} \rho(xyz)e^{2\pi i(\frac{h'x}{a}+\frac{k'y}{b}+\frac{l'z}{c})}.\frac{Vdxdydz}{abc}$$

Substituting the Fourier series for $\rho(xyz)$, every term vanishes on integration except the term for which

$$h = -h',\ k = -k',\ l = -l'$$

which integrates to $V.A'_{\bar{h}'\bar{k}'\bar{l}'}$ It follows that

$$F_{hkl} = A'_{\bar{h}\bar{k}\bar{l}}.V$$

$$F_{\bar{h}\bar{k}\bar{l}} = A'_{hkl}.V$$

where V is the unit cell volume. The density is then given by a triple Fourier series in which the Fourier coefficients are the structure factors F_{hkl}

$$\rho(x,y,z) = \frac{1}{V}\sum_{-\infty}^{\infty}\sum_{-\infty}^{\infty}\sum_{-\infty}^{\infty} F_{hkl}e^{-2\pi i(hx/a+ky/b+lz/c)}$$

Each hkl-reflection corresponds to a term in the Fourier representation of the electron density. In the case where all matter scatters with the same phase change ρ is everywhere real. In this case A'_{hkl} and $A'_{\bar{h}\bar{k}\bar{l}}$ are conjugate as are F_{hkl} and $F_{\bar{h}\bar{k}\bar{l}}$ the imaginary terms then cancel out in the expression for ρ. F_{hkl} and $F_{\bar{h}\bar{k}\bar{l}}$ represent the amplitude and phase of the diffracted beam with the phase referred to the chosen origin in the crystal. For crystals having a centre of symmetry, $F_{hkl} = F_{\bar{h}\bar{k}\bar{l}}$and

$$\rho(xyz) = \frac{1}{V}\sum_{-\infty}^{\infty}\sum_{-\infty}^{\infty}\sum_{-\infty}^{\infty} F_{hkl}cos2\pi(h\frac{x}{a}+k\frac{y}{b}+l\frac{z}{c})$$

Although equation 1 appears to offer a method for structure determination with atomic positions indicated by electron density peaks, the experimental value measured is an integrated intensity proportional to F^2_{hkl} even if all the F_{hkl} are real, such as when a centre of inversion is used as the origin. The sign of F_{hkl}, which represents the phase is unknown. However an approximate preliminary analysis of the positions of important atoms in the structure can determine which sign is correct. If the structure contains a few heavy atoms whose positions are known from space group requirements, the phase of the contribution from these atoms is then known and this determines the phases for most F_{hkl}. Other relationships between intensities and structure factor signs exist which enable the signs of all F_{hkl} to be determined, though this is very much an active field of research in which developments are continuously being made.

Representation of a structure can be obtained by forming a double Fourier series. Using measured reflections around a crystal zone in a double Fourier series gives electron density per unit area in a plane projection of the crystal structure. The resulting electron density map shows the crystal structure viewed along the zone axis. One to two hundred terms in the Fourier series are required to give a close representation of the structure. The two dimensional electron density is given by

$$\rho(xyz) = \frac{1}{A}\sum_{-\infty}^{\infty}\sum_{-\infty}^{\infty} F_{0kl}e^{-2\pi i(ky/b+lz/c)}$$

The results are represented by joining points of equal density like contour lines with atoms shown by 'peaks' surrounded by concentric contours such as the structure projection of ger-

anylamine hydrochloride shown in Figure 9.

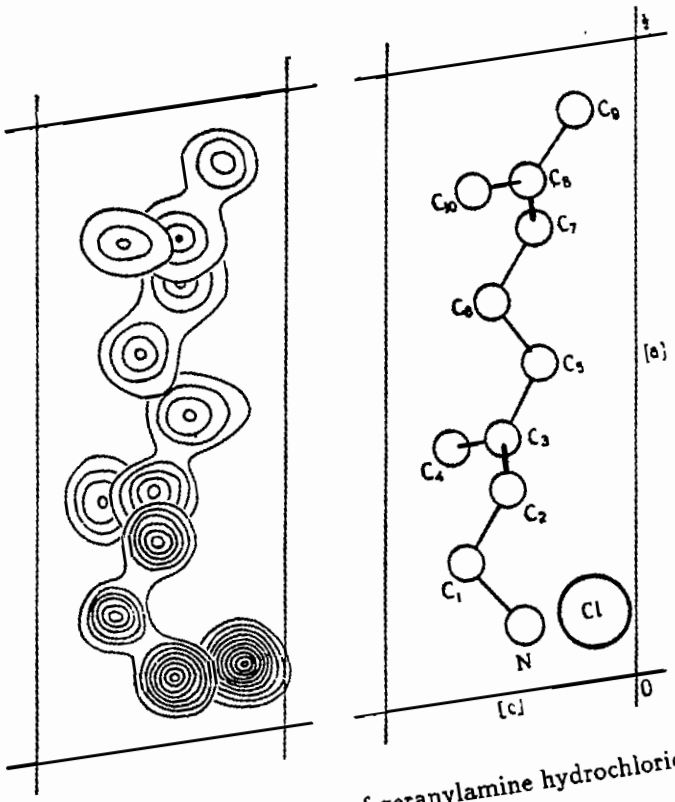

Fig. 9 Electron density map of geranylamine hydrochloride

2 Analysing Film Data

In summary, data analysis using the Laue method involves the following steps;

(a)microdensitometry of the films
(b)predicting a pattern from a known orientation and comparing with film to determine actual orientation
(c)refinement of the cell and orientation parameters to obtain accurate positional parameters for the spots on the given film
(d)integration of the film optical densities at the predicted positions for all the films in the pack
(e)determining inter-film scale factors, scaling together of the films in each pack and applying Lorentz, polarisation and obliquity corrections
(f) unscrambling of reflection intensities which are harmonic overlaps (multiples)
(g)normalisation of the intensities to take account of the variation of incident intensity with wavelength and other wavelength dependent factors, by internal comparisons

A series of programs have been developed at Daresbury for the quantitative analysis covering steps (b) to (f) of Laue patterns recorded on X-ray film.

2.1 Microdensitometry

A grain of silver in the emulsion of X-ray film becomes developable when it has been struck by a single X-ray quantum. It can be shown that as a consequence of this 'single hit process', the optical density of exposed and developed X-ray film is proportional to the incident X-ray intensity up to X-ray optical densities of at least 1.0.

The optical density is determined by measuring the ratio of transmitted to incident light, I_T/I_O, when white light falls on the film;

$$I_T = I_O 10^{-O.D.} \text{ or } O.D. = -log I_T/I_O \qquad (2)$$

A microdensitometer is used to measure the optical density over very small areas of the film.

The light not transmitted has been removed by true absorption and scattering away from the beam direction. If no scattered light is measured due to a small detector acceptance angle the instrument determines 'specular optical density'. If all scattered light is measured, the instrument determines 'diffuse optical density'.

The quantity with which single crystal diffraction work is concerned is the integrated intensity of the diffraction spots. This requires the determination of $\int^A O.D.\, dA$ over the area A of the spot. It is not permissable due to the logarithmic relationship of equation (1) to measure $\int^A I_T\, dA$ as density over the area of the spot is not constant. The integral $\int^A O.D.\, dA$ is always evaluated as $\sum O.D.$.

The number of spots over which a single diffraction spot is sampled is usually at least 50, for adequate accuracy for spots with steeply sloping density profiles. The quantity referred to somewhat incorrectly as the integrated intensity of a spot is then obtained by subtracting from the $\sum O.D.$ a similar sum measured over a background area which is a frame of elements surrounding the diffraction spot. The difference yields a quantity proportional to the true integrated intensity of the beam which produced the spot only after multiplication by a number of geometrical factors.

A rotating drum scanner has a rotating drum upon which the film is mounted. The x-axis is defined as the long axis of the drum about which it rotates, with y-axis around the drum circumference. The y-position of a datum is indicated by a rotary encoder attached to the

drum spindle and the x-position is that of the optical source outside the drum and the optical detector inside the drum. The source and detector are mounted on a carriage driven by a leadscrew and stepper motor parallel to the drum spindle. During a scan all the y-position readings on one x-position are taken in one revolution of the drum. The stepper motor advances the carriage to the next x-position to record the next set of y-readings. The scanner has a transparent acrylic drum to which films are attached by means of masking tape over the edges, and a silicon photo-diode detector for high stability and linearity.

The detector signals are digitised to 8-bit binary numbers representing optical density. The dynamic range can be chosen to correspond to one of 5 optical density ranges and there is an electronic offset to concentrate on the density region of interest. The source is a tungsten-halogen lamp with infrared filter. The apertures of the source and detector can be set either square or round and there are a variety of sizes. Both x and y axes of the scanner may be stepped in increments of 25, 50, 100 or 200 microns; called raster steps. Usually 2400 x 2400 raster points of (50 x 50)μm^2 size are scanned.

2.2 Pattern prediction and determination of missetting angles

We define X, Y and Z as orthogonal axes in reciprocal space. At any wavelength the reflecting sphere has a radius of $1/\lambda$. The figure shown below illustrates how reciprocal lattice point x, y, z projects as a Laue spot if diffraction conditions are met. The reciprocal lattice point lies on a reflecting sphere of radius |RF|, with centre $RF, 0, 0$ where;

$$\mathrm{RF} = (x^2 + y^2 + z^2)/2x$$

The coordinates of a diffraction spot on a flat film lying at some distance along the postive X-axis can be calculated. The Y and Z coordinates of the diffraction spot on the film YF and ZF (not shown), at a distance D from the crystal are merely projections of y and z values of the reciprocal lattice point at a distance $(-RF + x)$ is the scaling factor and;

$$XF = Dy/(-RF + x) \qquad \text{where } XF \text{ is parallel to } Y$$

$$YF = Dz/(-RF + x) \qquad \text{where } YF \text{ is parallel to } Z$$

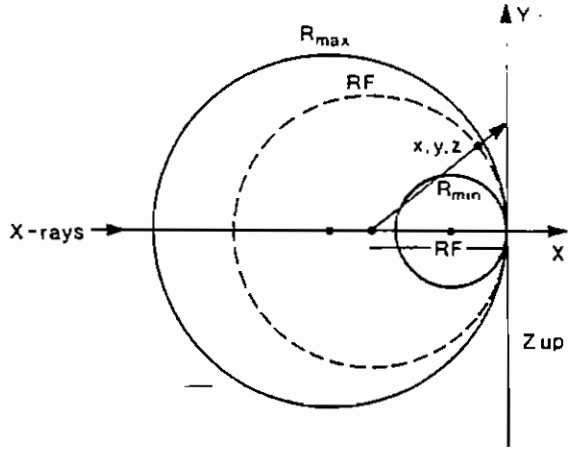

Fig.10 Reciprocal lattice point x, y, z gives rise to a Laue diffraction spot

The matrix $[A]$ relates to an ideal orientation of the reciprocal axes where for example $\mathbf{a}*$ is parallel to the X-ray beam and X and $\mathbf{c}*$ near to Z (in the XZ plane) for the monoclinic system;

$$[A] = \begin{bmatrix} \mathbf{a}* & 0 & \mathbf{c}*cos\beta* \\ 0 & \mathbf{b}* & 0 \\ 0 & 0 & \mathbf{c}*sin\beta* \end{bmatrix}$$

The matrix $[C]$ relates the real crystal orientation to this ideal setting by rotations ϕ_x, ϕ_y and ϕ_z about x, y and z;

$$[C] = \begin{bmatrix} cos\phi_z & -sin\phi_z & 0 \\ sin\phi_z & cos\phi_z & 0 \\ 0 & 0 & 1 \end{bmatrix} \begin{bmatrix} cos\phi_y & 0 & -sin\phi y \\ 0 & 1 & 0 \\ sin\phi_y & 0 & cos\phi_y \end{bmatrix} \begin{bmatrix} 1 & 0 & 0 \\ 0 & cos\phi_x & -sin\phi_x \\ 0 & sin\phi_x & cos\phi_x \end{bmatrix}$$

$$\begin{bmatrix} x \\ y \\ z \end{bmatrix} = [C][A] \begin{bmatrix} h \\ k \\ l \end{bmatrix}$$

A pattern is predicted using the reciprocal lattice cell dimensions, Bravais lattice type and angles ϕ_x, ϕ_y and ϕ_z to generate reciprocal lattice points within $1/d_{min}$ of the origin. The parameters $\lambda_{min}, \lambda_{max}$ and crystal to film distance D determine whether a reflection will be recorded. The recorded reflection position can be calculated and displayed on the screen. Other statistics determined are the numbers of reflections as a function of wavelength and the multiplicity.

The LAUE program is used to generate and display a Laue pattern determined from cell parameters, crystal to film distance, wavelength range, minimum d spacing, crystal type and setting. Alternatively, crystal orientation can be determined using the Auto-indexing command. To do this the SPOTIN program is used to pick nodal spots on a threshold plot to form a spot dump file. Indexing then works by matching the angles between reciprocal lattice vectors for these nodal spots against a table of angles of potential nodal spots prepared in advance from the crystal lattice parameters.

The routine works well provided the nodal indices are less than around 5 as the tabulation of angles is limited to those arising from a total of no more than about 280 vectors. The user is asked to supply a maximum value for $h^2 + k^2 + l^2$ to determine how many reciprocal lattice vectors are calculated. A low value speeds up the calculation but may miss some spots. A relatively high value should be used for non-primitive cells to make up for the systematically absent spots. The user is also prompted to supply an estimate of the error in spot positions of around 1 to 1.5 mm.

2.3 Refinement of Cell and Orientation Parameters

Once an initial orientation for the crystal has been determined it is necessary to refine this orientation and possibly the cell parameters before integration can proceed. The refinement is done by a numerical routine (NAG E04FDF). The routine minimises $\sum \delta^2$ for all spots in the list where

$$\delta = [(XF_{obs} - YF_{calc})^2 + (YF_{obs} - YF_{calc})^2]^{1/2}$$

and

XF_{obs}, YF_{obs} are the observed spot coordinates

XF_{calc}, YF_{calc} are the calculated spot coordinates

The program GENLAUE, which performs the refinement is used first with a predicted spot pattern superimposed on a film plot. Corresponding spots are then matched up by eye and the vector shifts are entered using the cursor. The numerical routine then minimises the set of shifts. Once the predicted pattern nearly coincides with film plot an automatic refinement is used. This refinement places boxes of a specified size at the predicted positions on the film and then determines the centre of gravity inside each box to give a set of vector shifts from the predicted position. GENLAUE produces two files which contain the values h, k, l, x, y, λ for each spot with space for the integrated intensities to be filled in.

2.4 Integration of Optical Densities

The program INTLAUE is used to evaluate integrated intensities from film data. The program divides a film into a number of bins and then uses profile fitting to obtain values of integrated intensity. Further final refinement is carried out in two stages prior to integration. First using spots near the centre of the film and then all spots. The spots used can be determined by setting the number used and then the intensity threshold at each stage to obtain a good distribution. The inner refinement produces an average spot profile indicating the most suitable box size for integration. Standard profiles are then evaluated based on singlet spots in 5,9 or 17 bins. Standard corrections for non-linear film response are made, and only reflections with intensities above a specified threshold on the previous film are measured on lower films in a pack. Figure 1 shows the measurement box used.

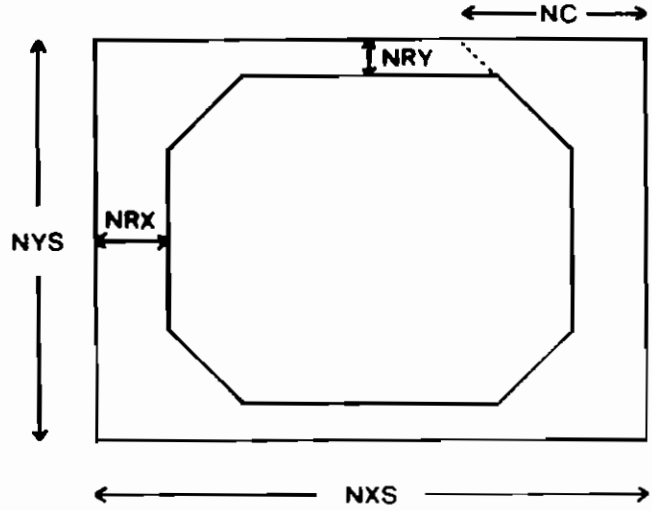

Fig. 11 Measurement box used for integration

NXS and NYS (odd integers) define the overall size of the measurement box in pixels. NRX and NRY define the widths of the background rim and NC defines the corner cutoff. The peak component of the measurement box is expanded automatically as function of Bragg angle to allow for increasing spot size due to oblique incidence of the diffracted beam on the film. The optical densities in the background region are fitted by a least squares plane. The constants a, b, c are determined by minimising $R1$ where;

$$R1 = \sum(\rho - ap - bq - c)^2$$

ρ denotes the optical density at the point with coordinates (p, q) with respect to the centre of the measurement box. The summation is over all the background pixels.

The value $P(p, q)$ of the standard profiles for each bin at the pixel with coordinates p,q is determined by minimising $R2$ where;

$$R2 = \sum_h [J_h P(p, q) - \rho_{corr}(p, q)]^2$$

minimisation gives;

$$P(p, q) = \frac{\sum J_h \rho_{corr}(p, q)}{\sum J_h^2}$$

J_h is the integrated intensity of the reflection, ρ_{corr} is the background corrected optical density and the summation extends over all contributing reflections. The profile fitted intensity is determined by finding the value of the scalar quantity J which provides the best least-squares

fit between the observed and scaled standard profiles;

$$R3 = \sum [JP - \rho_{corr}]^2$$

minimisation of $R3$ gives;

$$J = \frac{\sum P\rho_{corr}}{\sum P^2}$$

The profile fitted intensity I_p is then given by;

$$I_p = J \sum P = \frac{\sum P\rho_{corr} \cdot \sum P}{\sum P^2}$$

substituting $\rho_{corr} = \rho - ap - bq - c$ this becomes;

$$I_p = \frac{\sum \rho P - a\sum Pp - b\sum Pq - c\sum P}{\sum P^2} \cdot \sum P$$

For a given profile, all the summations except that involving ρP are constant for all reflections and need to be evaluated only once. Figure 12 shows a typical reflection peak in background.

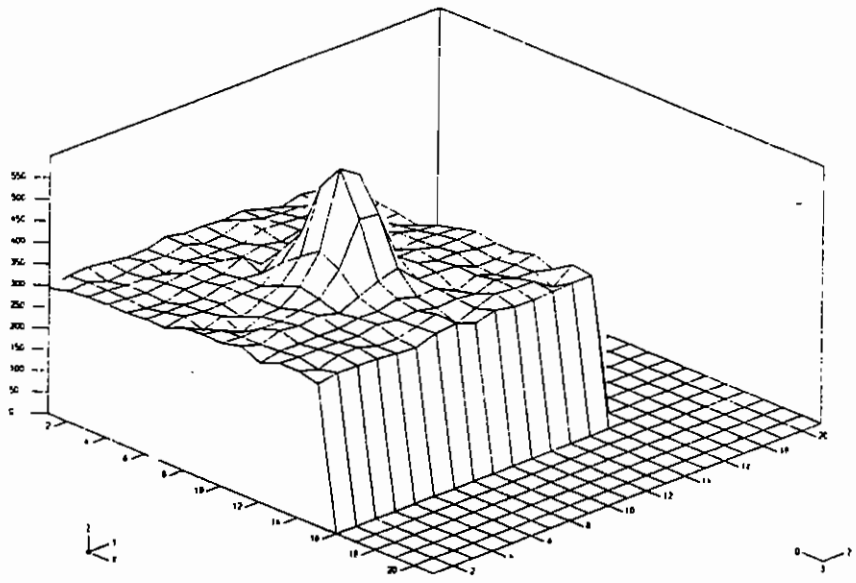

Fig. 12 Reflection peak in background

2.5 Scaling within a film pack

To be processable diffraction spots need to be recorded in the linear region of the film. This is the region where measured optical densities are directly proportional to intensities. A particular crystal has a range of intensities. The use of multiple films is needed to ensure that strong spots which overload the front film will be adequately recorded on subsequent films.

Film absorption is a function of wavelength. As the wavelength increases the difference between intensities of a reflection on adjacent films increases;

$$I_A/I_B = ke^{\alpha\lambda^3/cos2\theta}$$

It is necessary to correct data for film absorption. To do this the wavelengths are divided into three seperate ranges to eliminate reflections at the wavelengths of the silver and bromine absorption edges (0.48A<Ag<0.490A , 0.900A<Br<0.920A). Starting with the front two films in the pack, A and B, coefficients α are assigned for each of the three wavelength ranges based on a knowledge of film properties and then refined by an iterative procedure to give the best fit with the observed intensity values. Exclusion of data with large differences in intensity between adjacent films at short wavelengths produces a cleaner plot.

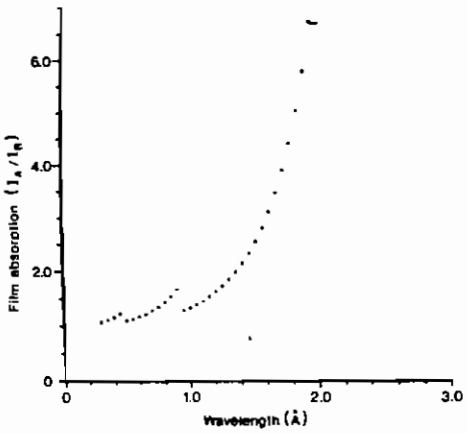

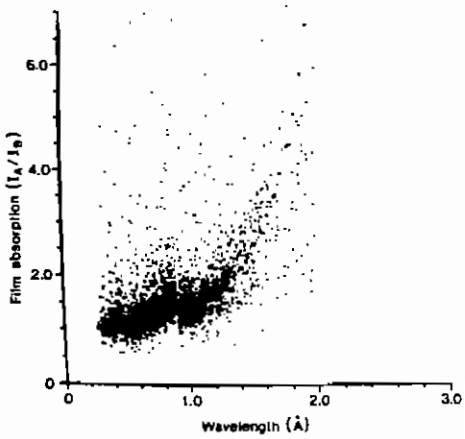

Fig. 13 Theoretical curve of film absorption as a function of wavelength

Measured film absorption as a function of wavelength.

The iteration procedure adjusts α to minimise the function;

$$\sum_{i=1}^{M}[(I_A/I_B)^{cos2\theta} - wKe^{\alpha\lambda^3}]^2$$

where M is the total number of reflections for which intensities are recorded on both films for each of the wavelength ranges and w is a weighting factor. Once this has been done reflections from lower films can be scaled up to the A film and averaged to give a single intensity for each reflection;

$$I_{mean} = \frac{\sum_i I_i/\sigma_i^2}{\sum_i 1/\sigma_i^2}$$

The data is finally scaled to corrected for Lorentz, polarisation, obliquity and the presence of two sheets of paper by;

$$ke(0.105/cos2\theta)/LP$$

where;

$$L = 1/sin^2\theta$$
$$P = \left(\frac{1+cos^2 2\theta}{2}\right)\left(1 - \tau\left(\frac{cos2\phi sin^2 2\theta}{1+cos^2 2\theta}\right)\right)$$

and;

$$\phi = tan^{-1}(XF/YF)$$

τ=the degree of polarisation.

2.6 Normalisation of Wavelengths

Symmetry related reflections can be used to determine a normalisation curve to correct intensity measurements for;-

(a) The incident intensity in the SRS spectrum. The long wavelengths in the spectrum are truncated as the beam passes through beam-line windows or any air paths on its way to the sample. Short wavelengths are cut off if a reflecting mirror is used.
(b) Sample absorption also truncates the long wavelengths.
(c) Film response. Bromine and silver K absorption edges improve the film efficiency in wavelength region where it is decreasing.
(d) The factor λ^4 in the formula for the integrated power

Symmetry related reflections should be recorded at the same intensity once wavelength dependent, intensity varying, factors have been corrected for, and assuming no anomalous dispersion. This fact enables scale factors to be determined for all wavelengths. A set of symmetry related reflections will be recorded at different wavelengths. The reflections will therefore sample different points of the wavelength normalisation curve and be recorded with different intensities. The amount of scaling that is required to increase the intensities of the different reflections to a reference value is determined. It is possible to use reflection intensities measured in one wavelength interval to serve as a reference and then scale all other wavelength intervals (bins) to that one. $f(\lambda)$, the wavelength normalisation curve, is set initially to 1.0 for each range. It is then improved by cycles of iteration until convergence is reached. A polynomial is then fitted to $f(\lambda)$ within each range, so that the normalisation value can be interpolated for values of λ between the range means.

3 Structural determination of ruby at high temperature and pressure

In the fields of material science, solid state physics, chemistry and geology problems involving crystalline matter at extreme conditions of temperarure and pressure occur routinely. Geologists are concerned with oxide and silicate structures during their formation, solid state physicists and chemists may study the variation of electronic structure and bonding with pressure and temperature while material scientists are interested in phase transitions.

Empirical descriptions of structural variation with temperature, pressure and composition are necessary for predicting the behaviour of materials at conditions not yet studied or unattainable in the laboratory. Such models may predict variation in structure or material properties such as molar volume at conditions existing in the earth's mantle for example.

Although the collection and analysis of data at non-ambient conditions is generally, technically more difficult the structural equations of state obtained provide important data on theoretical and applied problems in solid state science.

3.1 Experimental outline

We have collected and analysed data from ruby (corundum structure, Chromium doped) at ambient, 100°C, 380°C, 6.2kbar and 24.9kbar using the Laue technique. The ambient and high temperature data sets were collected using the same crystal in a high temperature furnace and the high pressure data was collected in a diamond anvil cell using a second crystal. The diffraction patterns were recorded on CEA Reflex 25 double sided emulsion film. Packs of six films were used with no foils between films. The crystal was larger than the beam cross-section so the irradiated cross section was 0.2mm. The crystal system is hexagonal. Figure 14 shows the experimental arrangement used.

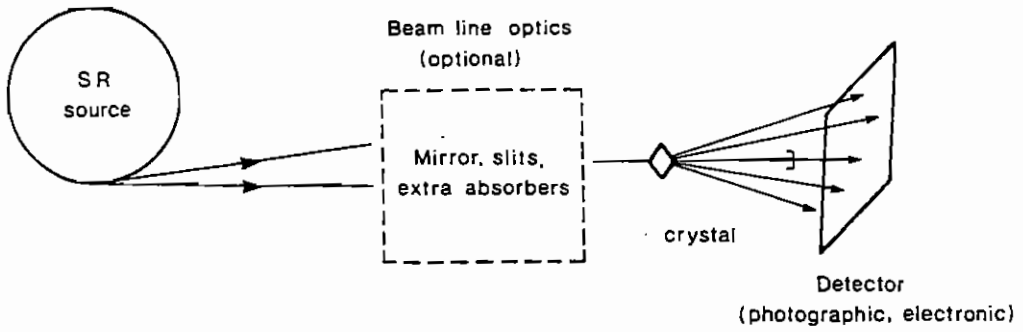

Fig. 14 Experimental arrangement

The following tables describe the pack sequences used in collecting the data. μ is the vertical camera rotation axis and ϕ is the horizontal rotation axis perpendicular to the beam direction. The first three pack sequences were collected with the SRS operaring in single bunch mode. The high pressure data was collected in multi-bunch mode.

RUBY 20.7°C 100mS exposure

Pack	μ	ϕ	Current(mA)	Distance(mm)
RC2AF	0°	0°	31.9	45
RC1AF	-5°	0°	31.9	45
RB3AF	-5°	10°	31.7	45
RC3AF	-5°	-10°	31.7	45
RB5AF	5°	-10°	31.6	53
RC4AF	5°	10°	31.6	53

RUBY $\approx$107° 100mS exposure

Pack	μ	ϕ	Current(mA)	Temp.(°C)	Distance(mm)
RZ1AF	0°	0°	29.7	107.9	45
RZ2AF	-5°	0°	29.5	108.1	45
RZ3AF	-5°	10°	29.5	108.0	45
RZ4AF	-5°	-10°	29.5	108.3	45
RZ5AF	5°	-10°	29.4	108.5	53
RZ6AF	5°	10°	29.4	108.5	53

RUBY $\approx$385° 100mS exposure

Pack	μ	ϕ	Current(mA)	Temp.(°C)	Distance(mm)
RY1AF	0°	0°	28.6	382.8	45
RY2AF	-5°	0°	28.4	383.8	45
RY3AF	-5°	10°	28.4	384.8	45
RY4AF	-5°	-10°	28.4	385.5	45
RY5AF	5°	-10°	28.3	386.2	53
RY6AF	5°	10°	28.3	386.8	53

RUBY 6.2kbar

Pack	μ	ϕ	Current(mA)	Time(mS)	Distance(mm)
RHP2AF	0°	0°	236.0	100	45
RHP1AF	0°	2°	230.9	80	45
RHP3AF	-1°	2°	230.2	80	45
RHP4AF	1°	-2°	228.8	80	45
RHP5AF	0°	1°	220.1	80	45

RUBY 24.9kbar

Pack	μ	ϕ	Current(mA)	Time(mS)	Distance(mm)
RHP6AF	0°	0°	213.4	80	45
RHP7AF	0°	2°	212.5	80	45
RHP9AF	1°	2°	204.5	60	45
RHP8AF	-1°	-2°	203.3	60	45
RHP10AF	-2°	-5°	202.3	60	45

3.2 Determination of crystal orientation

Figure 15 shows the nodal spots selected from the film RC1A to determine the missettting angles ϕ_x, ϕ_y, ϕ_z. The coordinates of these spots on the film were determined and a file containing the data was created using 'SPOTIN'. Vector angles in reciprocal space between the spots were determined and compared with tabulated angles to determine the missettting angles using 'NEWLAUE'. The remaining 6 orientation settings were routinely determined using this method. Figure 3 shows the computer simulated patterns for the 4 different orientations at the smaller crystal to film distance for the 20.7° data

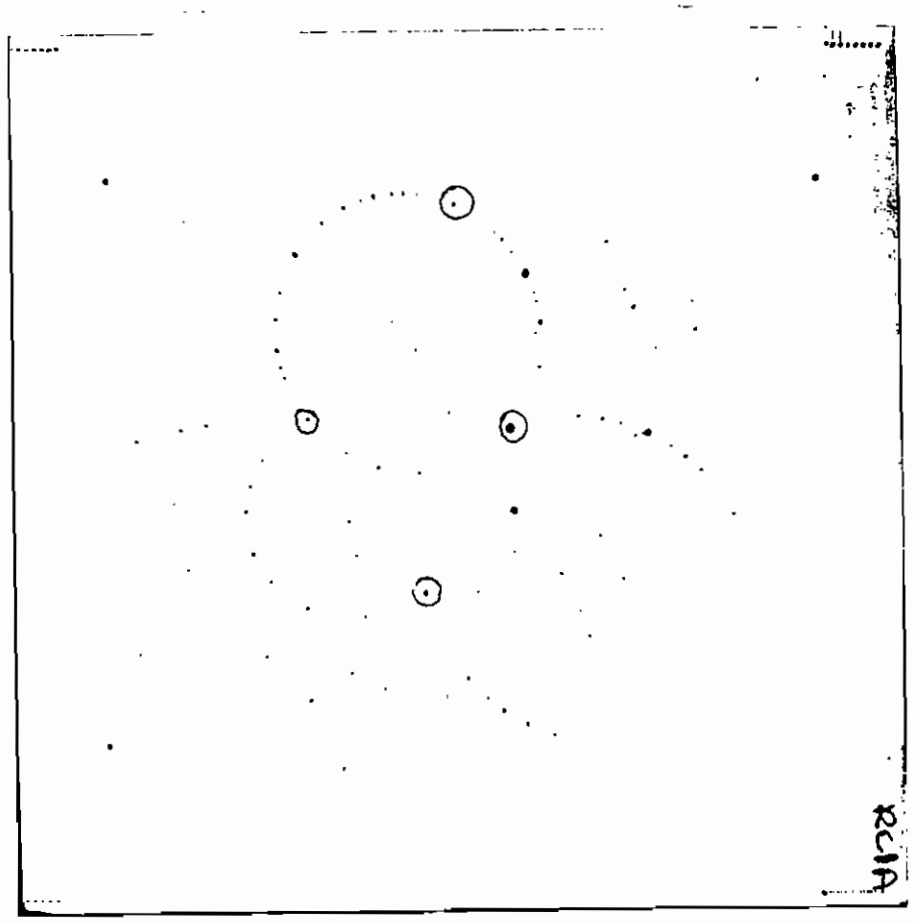

Fig. 15 RC1A nodal spots selected for indexing

3.3 Refinement of parameters

Once the initial crystal orientations had been determined 'GENLAUE' was used to refine the missetting angles, the crystal to film distance, the film centre and finally the c* lattice parameter of the reciprocal unit cell to give the best possible agreement between calculated and observed diffraction spot positions. Table 1 shows the final refined parameters and the number of spots generated. Table 2 gives the number of spots as a function of wavelength and their multiplicities.

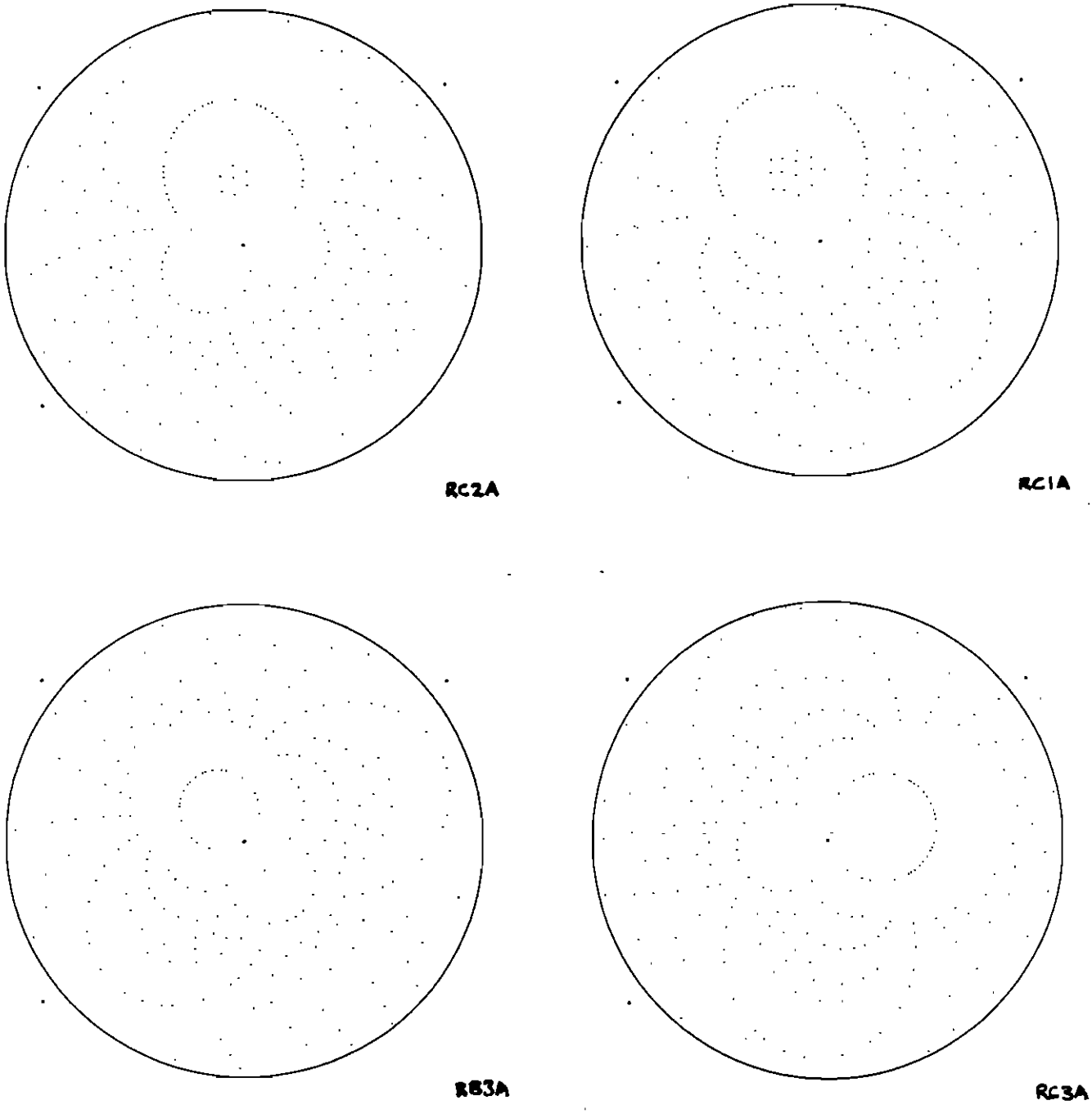

Fig. 16 Simulated patterns for Ruby at 20.7° (scale=0.65)

Table 1 Final refined parameters for Ruby at 20.7°

Pack	c-f(mm)	ϕ_x	ϕ_y	ϕ_z	Singlets	Multiplets	Nodals	Total
RC2AF	45.510	168.52	-1.68	152.34	171	25	180	196
RC1AF	45.558	168.42	-1.75	147.35	176	21	174	197
RB3AF	45.668	172.99	-10.67	146.91	178	24	177	202
RC3AF	45.549	163.47	6.90	147.10	179	21	174	200

Table 2 Analysis of spots generated

Multiplicity	RC2AF	RC1AF	RB3AF	RC3AF
1	174	181	178	179
2	16	13	15	15
3	4	3	5	2
4	3	2	3	2
5	2	2	1	1
6	0	1	0	1

λ_{max}	RC2AF	RC1AF	RB3AF	RC3AF
0.385	72	68	70	61
0.501	61	67	67	60
0.616	53	49	47	50
0.731	20	22	22	26
0.847	11	7	11	11
0.962	6	15	12	4
1.077	5	1	2	3
1.193	9	3	2	1
1.308	0	2	1	2
1.423	2	3	2	2
1.539	1	0	0	0
1.654	0	1	1	3
1.769	0	0	1	0
1.885	0	2	1	1
2.000	0	0	1	0

3.4 Integration

Integration of the spot optical densitites on each film was performed using 'INTLAUE'. The films were divided into 5 bins in order to give satisfactory profiles for each bin with approximately 15 to 25 spots in bins 1 to 4. Table 3 shows the number of spots integrated for each film. Harmonic overlaps (multiplets) were stored in a seperate file from singlets.

	Singlets		Multiplets				
Film	Measurable	Weak	Measurable	Weak	Measured	Overload	Total
RC2A	4	0	1	0	191	34	155
RC2B	3	83	1	3	106	27	77
RC2C	2	89	1	3	101	25	75
RC2D	2	95	1	3	95	22	77
RC2E	2	98	1	3	92	18	74
RC2F	2	104	1	3	86	15	71
RC1A	1	0	1	0	195	29	166
RC1B	1	95	1	3	97	27	70
RC1C	1	104	1	3	88	23	65
RC1D	1	112	1	3	80	22	57
RC1E	1	117	1	3	75	20	55
RC1F	1	117	1	3	75	16	59
RB3A	1	0	1	0	200	29	169
RB3B	1	94	0	7	100	28	69
RB3C	1	96	0	8	97	21	75
RB3D	1	100	0	8	93	18	75
RB3E	1	103	0	9	89	13	76
RB3F	1	107	0	9	85	12	73
RC3A	1	0	1	0	198	29	167
RC3B	1	89	1	3	106	29	75
RC3C	1	100	1	3	95	26	68
RC3D	1	102	1	3	94	20	74
RC3E	1	104	0	4	91	16	74
RC3F	1	110	0	4	85	10	75

Table 3 Spot integration results

3.5 Film scaling

Inter-film scaling to correct for film absorption, Lorentz, polarisation, obliquity and the paper in front of the film was performed using 'AFSCALE'. Table 4 shows the number of spots used for successive films in each pack to fit curves, and the overall R-factors obtained indicating the agreement between A-film intensities calculated from subsequent film scaling factors and actual A-film intensities.

Pack	A-B	B-C	C-D	D-E	E-F	R_{merge}	Spots
RC2AF	62	62	60	56	54	8.2	163
RC1AF	52	47	44	44	41	4.6	167
RB3AF	61	58	61	59	57	6.1	172
RC3AF	59	58	59	56	52	6.0	174

Table 4 Data points for scaling

3.6 Wavelength normalisation

The final step in obtaining a list of intensitites for each hkl reflection is normalising for wavelength dependent factors in the recorded intensity using 'LAUENORM'. Figure 17 shows the symmetry matrices used for the Ruby space-group $R\,\bar{3}\,c$ to determine reflections that are symmetry equivalents. The data from 4 packs was divided into 5 bins. Table 5 shows the number of reflections in each bin. Table 6 shows the numbers of reflections either recorded twice at different energies or as symmetery equivalents for each wavelength bin and for each pack.

$$\begin{bmatrix} -1 & 0 & 0 \\ 0 & -1 & 0 \\ 0 & 0 & -1 \end{bmatrix} \begin{bmatrix} -1 & -1 & 0 \\ 1 & 0 & 0 \\ 0 & 0 & 1 \end{bmatrix} \begin{bmatrix} 1 & 1 & 0 \\ -1 & 0 & 0 \\ 0 & 0 & -1 \end{bmatrix} \begin{bmatrix} 0 & 1 & 0 \\ -1 & -1 & 0 \\ 0 & 0 & 1 \end{bmatrix} \begin{bmatrix} 0 & -1 & 0 \\ 1 & 1 & 0 \\ 0 & 0 & -1 \end{bmatrix}$$

Fig. 17 Symmetry matrices for $R\,\bar{3}\,c$

Bin	Reflections	λ Range
1	50	0.270-0.313
2	61	0.313-0.356
3	60	0.356-0.400
4	51	0.400-0.443
5	59	0.443-0.486

Table 6 Wavelength bins data

Bin	1	2	3	4	5
1	6	10	15	11	10
2	10	7	13	16	18
3	15	13	10	13	19
4	11	16	13	6	13
5	10	18	19	13	7

Table 6 Wavelength bins overlap analysis

After scaling the following polynomial was fitted to the data. Figure 18 shows the normalised inverse λ curve plotted from this polynomial.

$$4420.07x^4 - 8377.23x^3 + 5931.87x^2 - 1862.50x + 219.30$$

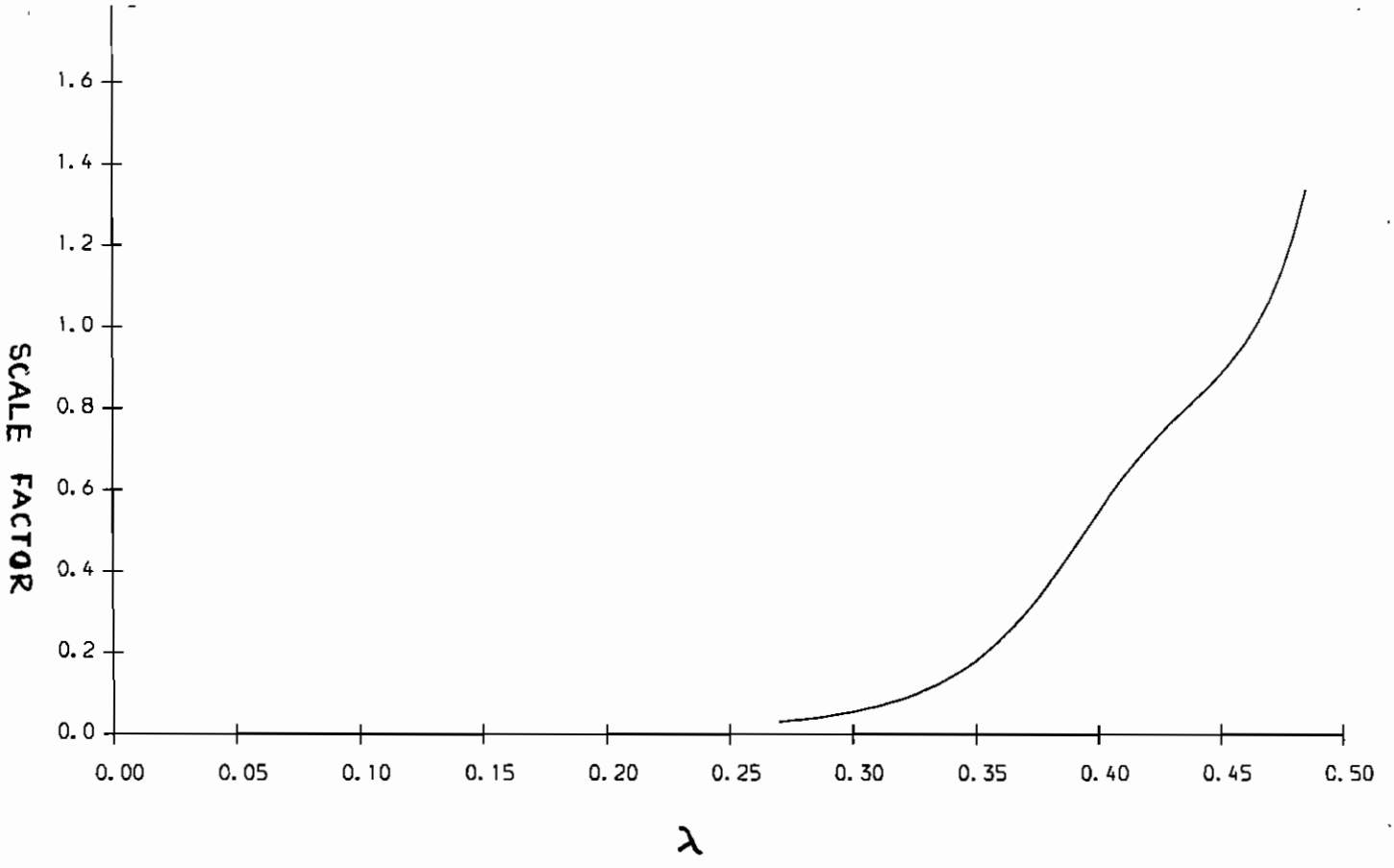

Fig. 18 Normalised inverse λ curve.

The normalisation curve was then fitted to all the data to produce a list of intensities and their standard deviations for all the *hkl* reflections. This analysis procedure was used for the data sets collected at $100°C$ and $380°C$ from the same sample. The high pressure data was collected from a smaller crystal in a Diacell Products diamond anvil cell. Figure 19 shows a diagram of the high pressure cell components. Most of the diffraction spots observed on the films were diamond diffraction spots and some of these overlapped the Ruby diffraction spots. It was therefore necessary to exclude these overlapping spots from the data set.

This was done by first determining the Ruby crystal orientation and refining the necessary variable parameters. Each spot position on the predicted diffraction pattern for the Ruby was then compared with the restored digitised image and the indices of any spot found to be overlapping were noted. the file containing the integrated intensities for each *hkl* produced by 'INTLAUE' was then edited and the standard deviations for overlapping spots set to 9999, flagging them as unusable data. Figure 20 shows the spots removed for the film RHP2A.

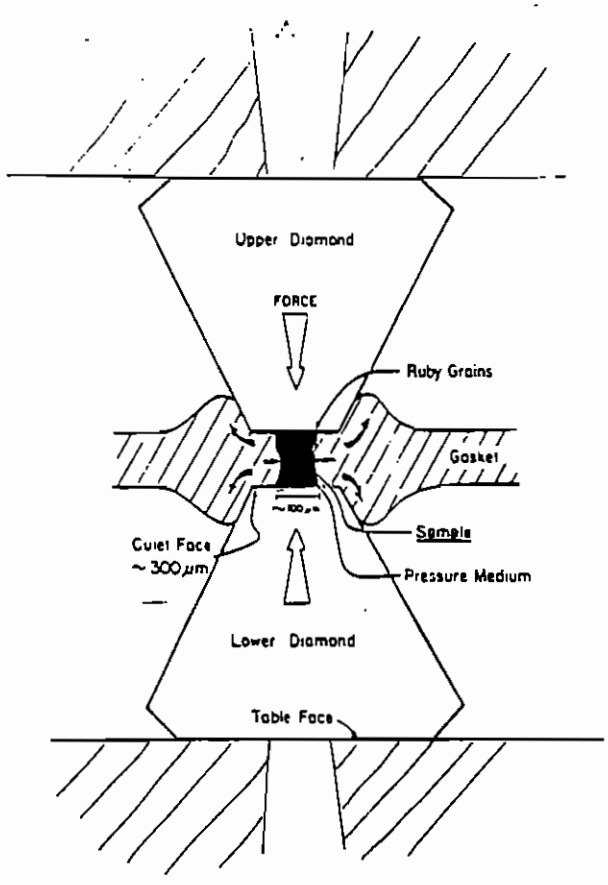

Fig. 19 Diamond anvil cell

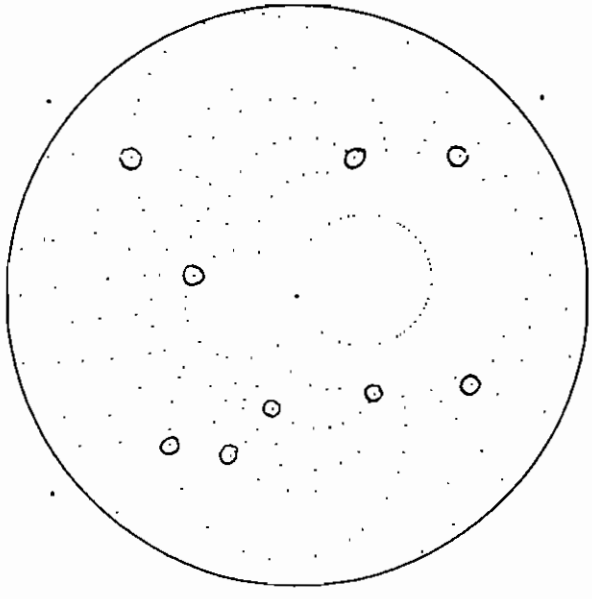

Fig.20 Overlapping diamond and ruby diffraction spots for RHP2A

3.7 Summary

The effects of temperature and pressure on the structure of Ruby are already well documented. The data for these previous studies having come from powder samples. The purpose of this experiment was to assess the potential for structure determination using the Laue technique. The well-known Ruby structure was chosen in order to compare actual structural determination results with those expected and estimate to what accuracy future structures could be resolved.

The last stage of the data analysis is the refinement of the known structure to obtain final atomic positional coordinates. This is done using 'SHELX-S' which is not part of the previous software analysis package developed at Daresbury. Though the final structural refinement is not yet complete, some preliminary analysis of the data has been performed using this program. Early results indicate differences between some calculated and observed structure factors. Determining the source of the error which appears to be systematic and may be a function of wavelength requires further investigation. Once resolved though, refinement of the structure should be a matter of routine.

Results to date are promising with good spatial resolution of the spot on the film, reasonable film scaling R-factors and more than enough spots being recorded within the dynamic range of the films to obtain a structural refinement. Many further possibilities exist for the technique in the future which may be inaccessible to other methods due to the rapid data collection times possible and hence the ability to monitor structural changes as they occur.

REFERENCES

(i) Arndt, U.W. & Wonacott, A.J. (1979) "The Rotation Method in Crystallography" Amsterdam: North Holland.

(ii) Bragg, W.L. (1949) 'The Crystalline State'

(iii) Campbell, J.W., Habash, J.,Helliwell, J.R., & Moffat, K. (1986) Information Quarterly for Protein Crystallography No. 18 Daresbury Laboratory

(iv) Helliwell, J.R., Habash, J., Cruickshank, D.W.J., Harding, M.M., Greenhough, T.J., Campbell, J.W., Clifton, I.J., Elder, M., Machin, P.A. Papiz, M.Z., Zurek, S. (1988) "The Recording and Analysis of Synchrotron X-radiation Laue Diffraction Photographs From the Pea Lectin and Small Molecule Crystals Using A Broad Wavelength Bandpass" DL/SCI/P558E

(v) Leslie, A. (1987) Proceedings of a Daresbury Study Weekend on "Protein Crystal Data Analysis" DL/SCI/R25

(vi) Machin, P.A. (1987) Proceedings of a Daresbury Study Weekend on "Protein Crystal Data Analysis" DL/SCIR25

(vii) Temple, B. & Moffat, K. (1987) Proceedings of a Daresbury Study Weekend on "Protein Crystal Data Analysis" DL/SCI/R25

(viii) Warren, B.E. (1969) "X-ray Diffraction"